Heme Biosynthesis

Subjects: Plant Sciences

Contributor: Jitka Richtová

Heme biosynthesis is essential for almost all living organisms. Despite its conserved function, the pathway's enzymes can be located in a remarkable diversity of cellular compartments in different organisms. This location does not always reflect their evolutionary origins, as might be expected from the history of their acquisition through endosymbiosis. Instead, the final subcellular localization of the enzyme reflects multiple factors, including evolutionary origin, demand for the product, availability of the substrate, and mechanism of pathway regulation. *Chromera velia* is a coral-associated alga bearing complex rhodophyte-derived plastid with a peculiar tetrapyrrole pathway. It synthesizes ALA using heterotrophic C4 path (same as apicomplexan parasites), which additionally supplies chlorophyll for photosystems. Using a combination of bioinformatics and experimental approaches, we investigated localizations of heme pathway enzymes in *C. velia*. Our data show that the pathway very likely starts in the mitochondrion, with the remaining enzymes located in the plastid. We demonstrate that the proteins are targeted to various cellular compartments by stringent translocon mechanisms that are not universal even for evolutionarily related organisms.

tetrapyrrole biosynthesis heterologous expression Chromera velia predictions

1. Introduction

Life as we know it would not be possible without tetrapyrroles, namely chlorophyll and heme. While chlorophyll is used exclusively in photosynthesis, heme can be involved in various electron transport chains and redox reactions [1]. Heme appears essential for almost all life on Earth, with only a few exceptions among pathogenic and anaerobic bacteria and a single exception in aerobic eukaryotes, the kinetoplastid *Phytomonas serpens* [2]. All other organisms either synthesize their own heme or obtain it from external sources [2]. Both heme and chlorophyll share a common synthetic pathway (up to protoporphyrinogen IX), which is well conserved among all three domains of life [3] (outlined in Figure 1). The first precursor of this pathway, 5-aminolevulinic acid (ALA), can be synthesized in two fundamentally different ways: primary heterotrophic eukaryotes and Alphaproteobacteria use the C4 (or Shemin) pathway, the condensation of succinyl-CoA and glycine, while Eubacteria, Archaea, and eukaryotic phototrophs form ALA from glutamate via a set of reactions termed the C5 pathway [4]. Eight molecules of ALA are assembled in three consecutive steps to uroporphyrinogen III, the first macrocyclic tetrapyrrole, which can convert to siroheme. Alternatively, the next three steps of the synthesis lead to protoporphyrinogen IX. In the chlorophyll synthesis branch, magnesium-chelatase inserts an Mg^{2+} ion into the center of the porphyrin ring. In the heme synthesis branch, insertion of a Fe^{2+} ion into the ring by ferrochelatase (FECH) finally completes the heme [1].

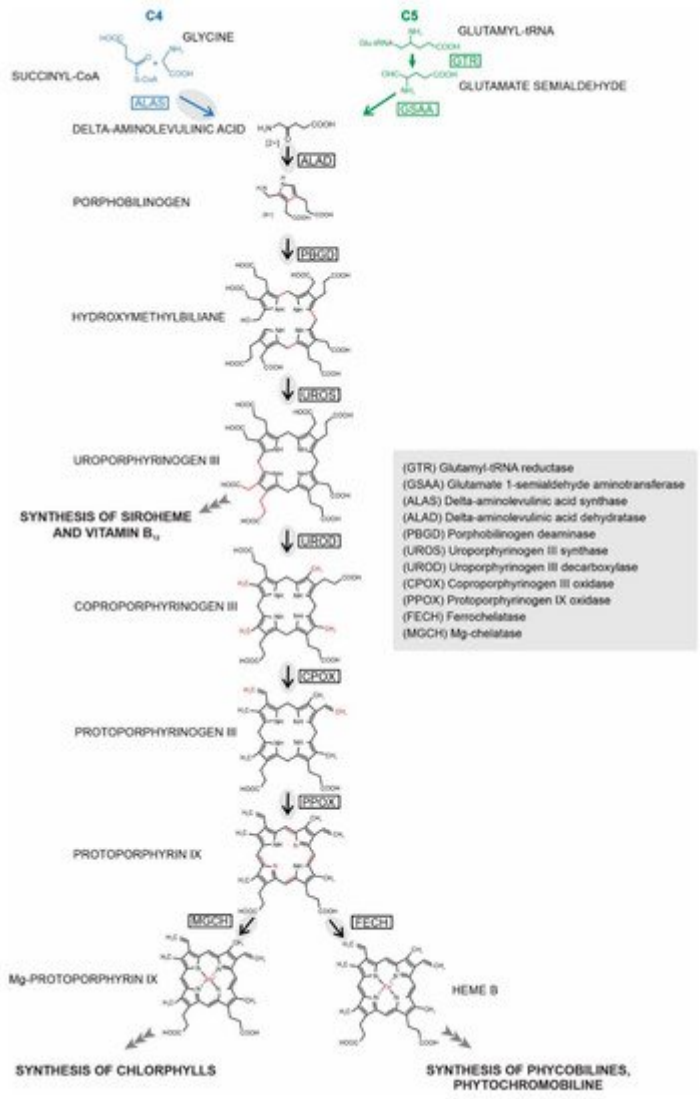

Figure 1. Tetrapyrrole synthesis. Enzymes working in particular synthesis steps are denoted by acronyms in boxes with their full names explained in the grey panel. Enzymatic steps (arrows) present in *C. velia* are in the grey oval. Changes in product structure are highlighted in red.

Tetrapyrrole biosynthesis in eukaryotes is largely influenced by past endosymbiotic events, in which mitochondria and plastids were acquired. This is reflected in the phylogenetic affinities of the associated genes, which often demonstrate similarity to homologous genes in Alphaproteobacteria or cyanobacteria, for mitochondrial or a plastid origin, respectively [4][5]. While the tetrapyrrole pathway is almost universally present, the subcellular distribution of the enzymes differs widely across the eukaryotic biodiversity. The location corresponds to the trophic strategy of the organism, cellular demand for the final products of the pathway, the evolutionary origin of the enzyme, and the need for tight regulation of the pathway [6][7][8][9][10].

In primary eukaryotic heterotrophs, both the initial and terminal steps of the synthesis take place in the mitochondria, which is not surprising considering the availability of the precursor, succinyl-CoA, and the demand for heme in the cytochromes of the respiratory chain [4][5][11]. The common location for the start and completion of heme synthesis is also important for the regulation of the pathway, which is mainly achieved by the heme-mediated

inhibition of ALA formation [6][7][8][9][10]. The middle part of the pathway in heterotrophs takes place in the cytosol, which necessitates the transport of ALA and a porphyrin intermediate across the mitochondrial membranes [12][13]. Most phototrophs use the C5 pathway to begin the tetrapyrrole synthesis. The whole process is located inside the plastid, the place with the highest demand for the final products, chlorophyll, and heme [14]. The euglenid alga *Euglena gracilis* [15] and the chlorarachniophyte *Bigelowiella natans* [16] possess both the plastid located (C5 based) pathway and the mitochondrially-cytosolic (C4 based) pathway. Apicomplexan parasites [17] such as *Plasmodium* or *Toxoplasma* harbor a non-photosynthetic relic plastid (the apicoplast) and possess a rather peculiar heme synthesis. The pathway starts via the C4 route in the mitochondrion; the next four steps are apicoplast localized, consecutively, coproporphyrinogen oxidase (CPOX) is active in the cytosol, and the synthesis is completed by protoporphyrinogen oxidase (PPOX) and FECH in the mitochondrion again [5][11][18][19][20][21]. Such complicated intracellular distribution of heme pathway enzymes most likely arose because of the transition from a photosynthetic to a parasitic lifestyle [5][11][20].

All tetrapyrrole pathway enzymes from the organisms mentioned above are encoded in the nucleus and hence must be targeted to a relevant compartment after translation in the cytosol. For that purpose, cells evolved various targeting signals that can be N-terminal or C-terminal extensions or lie internally within the protein [22]. For the transport through the ER, proteins are equipped with an N-terminal “signal peptide” (SP). Proteins targeted to plastids of primary phototrophs bear a “transit peptide” (TP) that is identified by translocons of outer and inner chloroplast membrane (TOC and TIC), respectively [23][24]. Complex plastids are coated with additional membranes; to pass them, proteins need a “bipartite targeting sequence” (BTS) consisting of an SP that is cleaved immediately after crossing the outermost membrane and a TP that escorts the protein to plastid stroma, where the TP is also excised to expose the mature protein [22][23][24][25][26].

Chromera velia is an alveolate alga belonging to the group Apicomonada [27], isolated from stony corals from Sydney Harbor in Australia [28]. Together with *Vitrella brassicaformis*, it represents the closest known phototrophic relative to apicomplexan parasites [29]. Like other Apicomplexa and algae with complex plastids, chromerids host rhodophyte-derived plastids surrounded by four membranes [28][29][30][31][32][33][34]. Although *C. velia* is a phototroph, it uses mitochondrially-located ALA synthase (ALAS) to synthesize ALA in the C4 route. All the C5 pathway enzymes found in other phototrophs are missing from chromerids [11]. The remaining enzymes of the pathway (from ALA to heme) display mosaic evolutionary origins (cyanobacterial, eukaryotic, and proteobacterial). Most of the enzymes involved in the pathway possess predicted bipartite targeting sequences (BTS) known to mediate the import of nuclear-encoded proteins into complex plastids [11][35][36].

To see how the pathway is organized in the photosynthetic chromerids and to better understand what evolutionary forces shaped the unusual pathway in Apicomplexa, we experimentally tested the locations of heme pathway enzymes in the *C. velia*. As there is no transfection system for *C. velia* yet, we decided to use the heterologous expression in a photosynthetic diatom and in an apicomplexan parasite. This also allowed insight into the compatibility of targeting mechanisms between diatoms and apicomplexans, including chromerids. The best-established transfection systems in organisms related to *C. velia* are those for the apicomplexans *Toxoplasma gondii* and *Plasmodium falciparum* and for the diatoms *Thalassiosira pseudonana* and *Phaeodactylum tricornutum*

[37][38][39][40][41]. Both groups of organisms, apicomplexans, and diatoms contain secondary plastids surrounded by four membranes, and their plastid targeting mechanisms have been extensively studied [23][42][43][44][45][46][47][48]. The apicomplexan parasites are more closely related to *C. velia*; however, the plastids in *C. velia* were hypothesized to originate from a tertiary endosymbiotic event with a stramenopile [29][33][34][49][50]. Moreover, diatoms and *C. velia* share a phototrophic lifestyle, which requires more complex regulation of the tetrapyrrole synthesis due to the presence of the chlorophyll branch [5][15][16].

2. Prediction of Localization of Heme Synthesis Enzymes in C. velia

Various bioinformatics tools can be used to predict N-terminal targeting presequences typically associated with targeting to specific subcellular compartments. We analyzed the predicted targeting of the *C. velia* heme pathway enzymes using the following algorithms: SignalP 4.1 [51] in combination with TargetP 1.1 [52], to determine the presence of bipartite targeting sequences (BTS). As *C. velia* hosts complex plastid surrounded by four membranes [28][31], we also took advantage of the ASAFind predictor, designed to predict protein targeting to rhodophyte-derived complex plastids [53]. We ran ASAFind combined with different versions of SignalP and also used the *C. velia* optimized predictor ASAFind+ [54] in conjunction with SignalP 4.1. For mitochondrial transit peptides, we also used the prediction method MitoFates [55].

According to SignalP 4.1 and TargetP 1.1, ALAS has no detectable ER signal peptide (ER-SP) or TP. This also applies to ALAD2 and UROS. Complete BTSs composed of SPs and TPs were found in ALAD1, porphobilinogen deaminase (PBGD), uroporphyrinogen decarboxylase 1 (UROD1), UROD2, both coproporphyrinogen oxidases (CPOX1, CPOX2), protoporphyrinogen oxidase 1 (PPOX1), and FECH1. ER-SPs without subsequent TP were found in UROD3 and FECH2. Mitochondrial TPs were detected in ALAD3 and PPOX2 by TargetP, while MitoFates predicted mitochondrial TPs for UROD1 and PPOX2. Due to the good prediction performance of SignalP- and TargetP- based methods in diatoms [53][56] and *C. velia* [54], we decided to weigh the results of SignalP/TargetP in conjunction with ASAFind or ASAFind+ higher than the MitoFates results.

All ASAFind predictions consistently suggested plastid localization for ALAD1, PBGD, UROD1, UROD2, UROD3, CPOX1, CPOX2, PPOX1, and FECH1. The remaining enzymes of the pathway appear to lack the ER-SP. The output of ASAFind and ASAFind+ combined with TargetP 2.0 agreed with the results mentioned above, except for FECH2, which according to TargetP 2.0, also has an ER-SP but no predicted plastid targeting by either ASAFind or ASAFind+. All above-mentioned predictors agreed on ALAS, ALAD2, and UROS lacking N-terminal targeting signal (Figure 2).

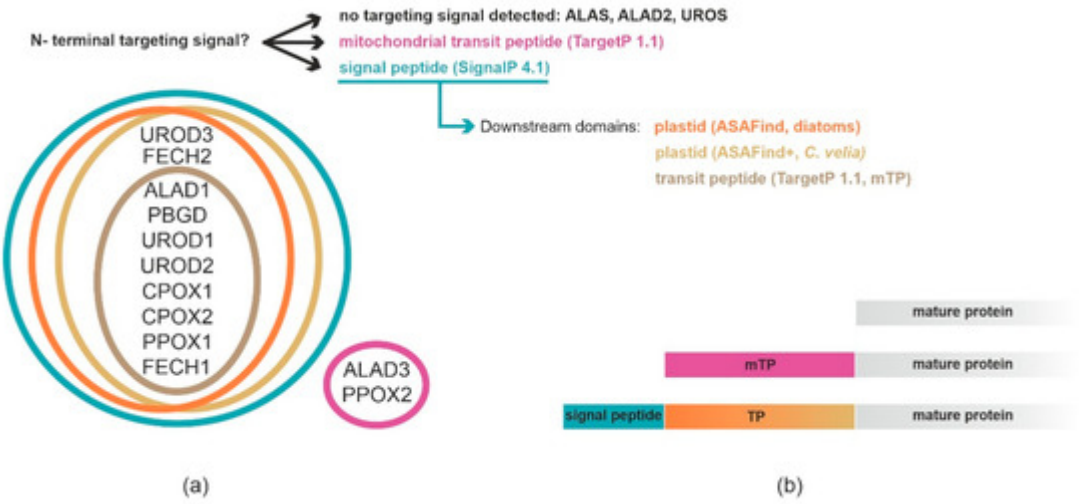

Figure 2. In silico targeting predictions for heme biosynthesis pathway enzymes in *C. velia*. (**a**) The Euler diagram displays the interpretation of targeting signals by various predictors. (**b**) Scheme showing different possibilities of N-terminal targeting signals.

We interpret the results as follows: ALAS, ALAD2 and UROS have no detectable targeting signal. ALAD3 and PPOX2 have TP (detected by TargetP 1.1). The remaining enzymes (ALAD1, PBGD, UROD1, UROD2, UROD3, CPOX1, CPOX2, PPOX1, and FECH1) were predicted to be plastid-targeted proteins by most of the used predictors.

3. Analyses of C. velia Heme Pathway Enzymes N-termini Sequence

We analyzed the N-terminus sequence of *C. velia* heme pathway enzymes with predicted BTS. We compared the aa distribution and overall net charge of these proteins with works already published on the set of plastid targeted proteins from diatoms [53] and *C. velia* [54]. We found that *C. velia* has about 50% lower frequency of serine and an overall higher proportion of positively charged residues within the first 20 aa of the TPs than diatoms (Figure 3). Seven of the nine predicted BTS of the *C. velia* enzymes of interest contain negatively charged residues that are almost absent in diatoms [53].

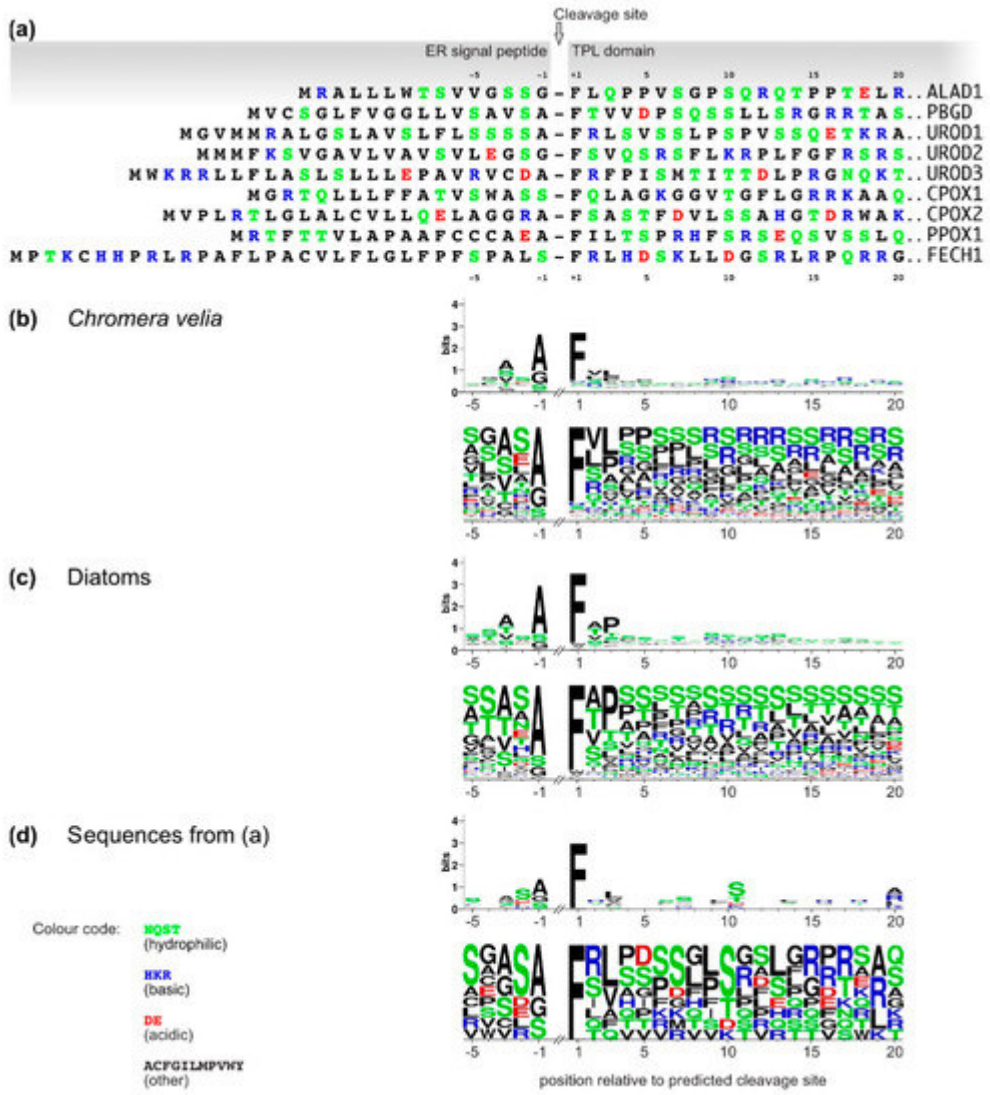

Figure 3. (**a**) ER-SP and TP domains of *C. velia* heme pathway enzymes. Coordinates are relative to the predicted SP cleavage site (arrow). Only enzymes that were positive for BTS are shown, amino acids in one-letter code, color code is identical for all panels. (**b**–**d**) Sequence logos (upper panels) and frequency plots (lower panels) of plastid targeting BTS cleavage site motifs and TPs from (**b**) *C. velia* (*n* = 146 data from [5]), (**c**) diatoms (*n* = 166, reproduced from [53]), and (**d**) the *C. velia*heme pathway enzymes shown in A (*n* = 9).

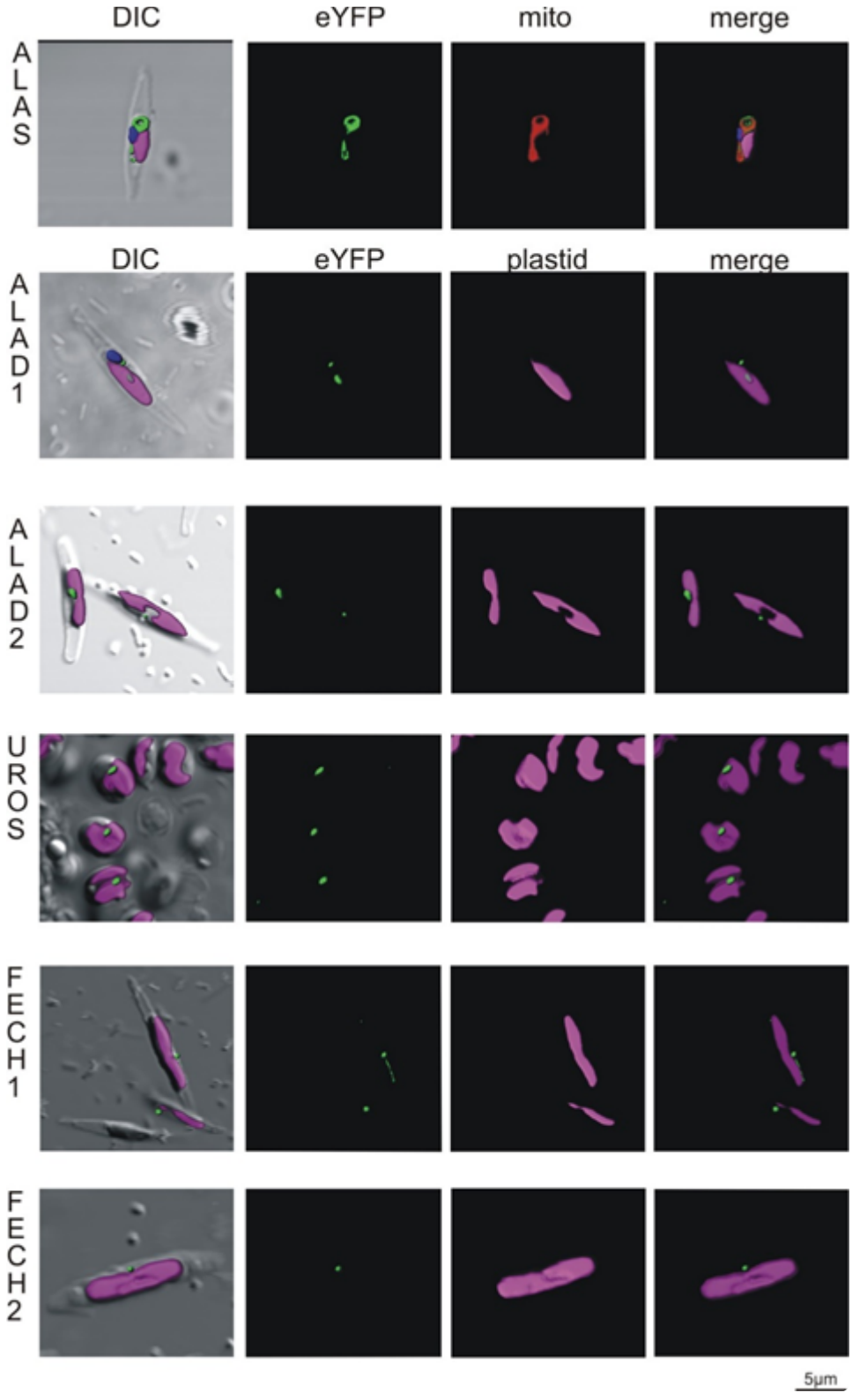

Figure 4. Heterologous expression of *Phaeodactylum tricornutum* with genes from *Chromera velia* heme pathway enzymes. Selected enzymes were tagged on their C-terminus by eYFP (green), magenta indicates plastid autofluorescence, MitoTracker® Orange CM-H2TMRos (ALAS, red) indicates mitochondrion. The Green eYFP signal of *C. velia* ALA synthase colocalizes with the red signal of *P. tricornutum* mitochondrion (row ALAS). Typical "blob-like" structures are found in heterologous expression of ALA dehydratases (ALAD1, ALAD2), uroporphyrinogen synthase (UROS), and both ferrochelatases (FECH1, FECH2).

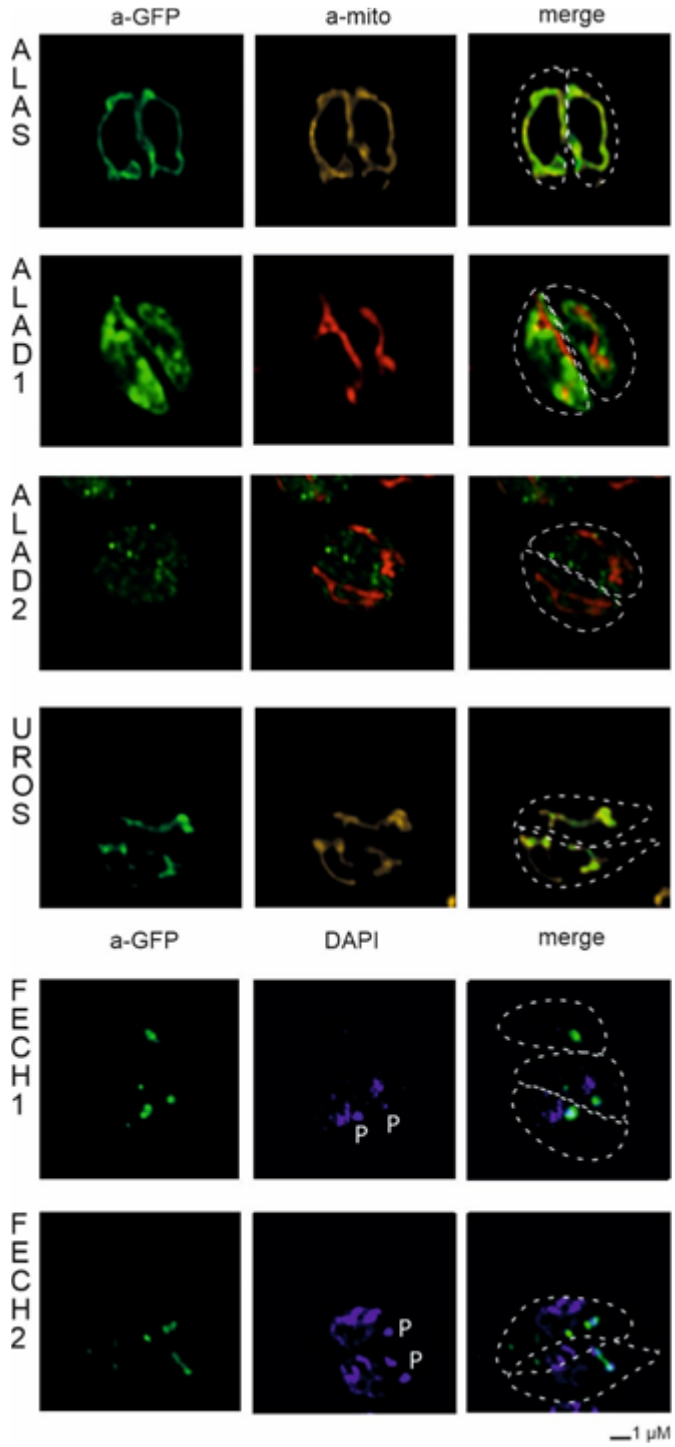

Figure 5. Heterologous expression of *Toxoplasma gondii* with genes from *Chromera velia* heme pathway enzymes. Immunofluorescence assays of transfected *T. gondii*, anti-GFP antibody were used to detect eYFP tagged *C. velia* enzymes. Anti-GFP (green) colocalized with mitochondrial anti-TgMys (a-mito, red and yellow) signal in case of ALAS and UROS. ALAD1 and ALAD2 signal were detected in the cytosol. FECH1 and FECH2 signal was found to overlap with DAPI (blue) signal at the area of parasite apicoplast. The apicoplast is denoted by "P." Dashed line indicates *T. gondii* cell border.

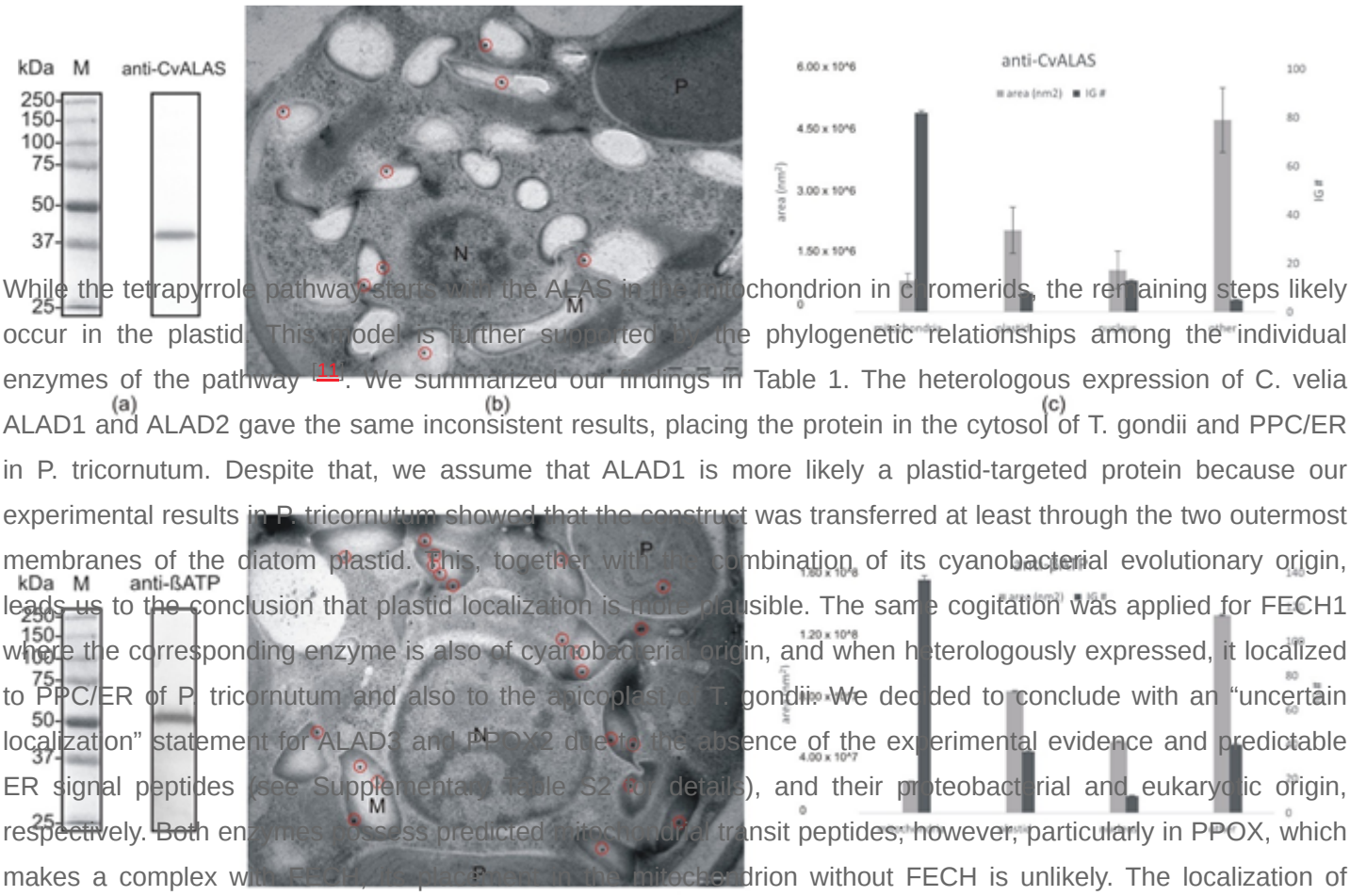

Figure 7. Immunogold labeling: (**a**) Western blot with anti-CvALAS on total protein extract from *C. velia* (**b**) Micrograph of *C. velia* ultrathin section after immunogold labeling with specific anti-CvALAS as a primary antibody. The majority of gold particles (encircled) were detected in the mitochondria. (**c**) Distribution of secondary IG particles (detecting anti-CvALAS) among cell compartments counted from all 35 micrographs. (**d**) Western blot with anti-βATP on total protein extract from *C. velia* (**e**) Micrograph of *C. velia* ultrathin section after immunogold labeling with specific anti-βATP as a primary antibody. The majority of gold particles (encircled) were detected in *C. velia* mitochondria. (**f**) Distribution of secondary IG particles (detecting anti-βATP) among cell compartments counted from all 35 micrographs. N = nucleus, M = mitochondria, P = plastid.

While the tetrapyrrole pathway starts with the ALAS in the mitochondrion in chromerids, the remaining steps likely occur in the plastid. This model is further supported by the phylogenetic relationships among the individual enzymes of the pathway [11]. We summarized our findings in Table 1. The heterologous expression of C. velia ALAD1 and ALAD2 gave the same inconsistent results, placing the protein in the cytosol of T. gondii and PPC/ER in P. tricornutum. Despite that, we assume that ALAD1 is more likely a plastid-targeted protein because our experimental results in P. tricornutum showed that the construct was transferred at least through the two outermost membranes of the diatom plastid. This, together with the combination of its cyanobacterial evolutionary origin, leads us to the conclusion that plastid localization is more plausible. The same cogitation was applied for FECH1 where the corresponding enzyme is also of cyanobacterial origin, and when heterologously expressed, it localized to PPC/ER of P. tricornutum and also to the apicoplast of T. gondii. We decided to conclude with an "uncertain localization" statement for ALAD3 and PPOX2 due to the absence of the experimental evidence and predictable ER signal peptides (see Supplementary Table S2 for details), and their proteobacterial and eukaryotic origin, respectively. Both enzymes possess predicted bipartite mitochondrial transit peptides; however, particularly in PPOX, which makes a complex with FECH, the presence in the mitochondrion without FECH is unlikely. The localization of ALAD3 in the mitochondrion and a formation of porphobilinogen in this organelle would require additional transport of porphobilinogen to the plastid over the four membraned envelopes. The remaining enzymes (PBGD, UROD1, UROD2, UROD3, CPOX1, CPOX2, and PPOX1) were concluded as "plastid" localized due to the congruency of the prediction result. However, spatial separation of the beginning and the end of the pathway is unprecedented, and it would require regulatory mechanisms that are not yet known. Therefore, we cannot rule out the possibility of recent reassignments of intracellular locations or dual targeting of the enzymes. Our work on localization of C. velia heme pathway enzymes shows that the subcellular localization of biosynthetic pathway within any organism is a concert of multiple factors rather than a solo for one major element.

Enzyme	Accession (CryptoDB)	Evolutionary origin	Targeting prediction	Localization *T. gondii*	Localization *P. tricornutum*	Conclusion
ALAS	Cvel_28814.t1	Alphaproteobacteria	No targeting signal identified	Mitochondria	Mitochondria	Mitochondria

07, 58,
Ayala,
ty.
3. Jordan, P.M. Highlights in haem biosynthesis. Curr. Opin. Struct. Biol. 1994, 4, 902–911.

ALAD1	Cvel_108.t1	Cyanobacteria	Plastid	Cytosol	PPC/ER	Plastid	
ALAD2	Cvel_13826.t1	Primary alga	No targeting signal identified	Cytosol	PPC/ER	Uncertain location	
ALAD3	Cvel_36189.t1	Proteobacterial	Mitochondria	Not tested	Not tested	Uncertain location	
PBGD	Cvel_26028.t1	Alphaproteobacteria	Plastid	Not tested	Not tested	Plastid	
UROS	Cvel_15018.t1	Uncertain origin in primary alga	No targeting signal identified	Mitochondria	PPC/ER	Uncertain location	
UROD1	Cvel_14720.t1	Cyanobacteria	Plastid	Not tested	Not tested	Plastid	
UROD2	Cvel_5098.t1	Endosymbiont nucleus	Plastid	Not tested	Not tested	Plastid	
UROD3	Cvel_31936.t1	Secondary host nucleus	Plastid	Not tested	Not tested	Plastid	
CPOX1	Cvel_21486.t1	Secondary host nucleus	Plastid	Not tested	Not tested	Plastid	
CPOX2	Cvel_2641.t1	Uncertain origin in primary alga	Plastid	Not tested	Not tested	Plastid	
PPOX1	Cvel_13840.t1	Cyanobacteria	Plastid	Not tested	Not tested	Plastid	

Protists; Archibald, J.M., Simpson, A.G.B., Slamovits, C.H., Eds.; Springer International Publishing: Cham, Switzerland, 2017; pp. 567–624.

18. Ralph, S.A.; Van Dooren, G.G.; Waller, R.; Crawford, M.J.; Fraunholz, M.; Foth, B.J.; Tonkin, C.J.; Roos, D.; McFadden, G.I. Metabolic maps and functions of the Plasmodium falciparum apicoplast. Nat. Rev. Microbiol. 2004, 2, 203–216.

PPOX2	Cvel_18037.t1	Eukaryotic origin	Mitochondria	Not tested	Not tested	Uncertain location
FECH1	Cvel_18167.t1	Cyanobacteria	Plastid	Apicoplast	PPC/ER	Plastid
FECH2	Cvel_26873.t1	Alphaproteobacteria	Signal peptide positive	Apicoplast	PPC/ER	Uncertain location

Table shows results described in the manuscript. Enzymes are listed according to their order during the synthesis of heme. The evolutionary origins of each of the enzymes are based on phylogenetic analyses from the work of [11][16]. The last column of the table contains our hypothetical conclusions about the *C. velia* enzyme localization based on our findings.

Press: Cambridge, MA, USA, 2002; 336p.

23. Kroth, P.G. Protein transport into secondary plastids and the evolution of primary and secondary plastids. Int. Rev. Cytol. 2002, 221, 191–255.

24. Gould, S.B.; Waller, R.; McFadden, G.I. Plastid evolution. Annu. Rev. Plant Biol. 2008, 59, 491–517.

25. Bolte, K.; Bullmann, L.; Hempel, F.; Bozarth, A.; Zauner, S.; Maier, U.G. Protein targeting into secondary plastids. J. Eukaryot. Microbiol. 2009, 56, 9–15.

26. Maier, U.G.; Zauner, S.; Hempel, F. Protein import into complex plastids: Cellular organization of higher complexity. Eur. J. Cell Biol. 2015, 94, 340–348.

27. Cavalier-Smith, T. Kingdom Chromista and its eight phyla: A new synthesis emphasising periplastid protein targeting, cytoskeletal and periplastid evolution, and ancient divergences. Protoplasma 2018, 255, 297–357.

28. Moore, R.B.; Oborník, M.; Janouškovec, J.; Chrudimský, T.; Vancová, M.; Green, D.H.; Wright, S.W.; Davies, N.W.; Bolch, C.J.S.; Heimann, K.; et al. A photosynthetic alveolate closely related to apicomplexan parasites. Nature 2008, 451, 959–963.

29. Oborník, M.; Modrý, D.; Lukeš, M.; Černotíková-Stříbrná, E.; Cihlář, J.; Tesařová, M.; Kotabová, E.; Vancová, M.; Prasil, O.; Lukeš, J. Morphology, ultrastructure and life cycle of Vitrella brassicaformis n. sp., n. gen., a novel chromerid from the Great Barrier Reef. Protist 2012, 163, 306–323.

30. Janouškovec, J.; Tikhonenkov, D.; Burki, F.; Howe, A.T.; Kolísko, M.; Mylnikov, A.P.; Keeling, P.J. Factors mediating plastid dependency and the origins of parasitism in apicomplexans and their close relatives. Proc. Natl. Acad. Sci. USA 2015, 112, 10200–10207.

31. Oborník, M.; Kručinská, J.; Esson, H. Life cycles of chromerids resemble those of colpodellids and apicomplexan parasites. Perspect. Phycol. 2016, 3, 21–27.

32. Füssy, Z.; Masařová, P.; Kručinská, J.; Esson, H.J.; Oborník, M. Budding of the alveolate alga Vitrella brassicaformis resembles sexual and asexual processes in apicomplexan parasites.

Protist 2017, 168, 80–91.

33. Oborník, M. Endosymbiotic evolution of algae, secondary heterotrophy and parasitism. Biomolecules 2019, 9, 266.
34. Oborník, M. Photoparasitism as an intermediate state in the evolution of apicomplexan parasites. Trends Parasitol. 2020, 36, 727–734.
35. Kilian, O.; Kroth, P.G. Identification and characterization of a new conserved motif within the presequence of proteins targeted into complex diatom plastids. Plant J. 2005, 41, 175–183.
36. Patron, N.J.; Waller, R. Transit peptide diversity and divergence: A global analysis of plastid targeting signals. BioEssays 2007, 29, 1048–1058.
37. Apt, K.E.; Grossman, A.R.; Kroth-Pancic, P.G. Stable nuclear transformation of the diatom Phaeodactylum tricornutum. Mol. Gen. Genet. MGG 1996, 252, 572–579.
38. Striepen, B.; He, C.Y.; Matrajt, M.; Soldati-Favre, D.; Roos, D. Expression, selection, and organellar targeting of the green fluorescent protein in Toxoplasma gondii. Mol. Biochem. Parasitol. 1998, 92, 325–338.
39. Poulsen, N.; Chesley, P.M.; Kröger, N. MOLECULAR genetic manipulation of the diatom Thalassiosira pseudonana (bacillariophyceae). J. Phycol. 2006, 42, 1059–1065.
40. Striepen, B.; Soldati, D. Genetic manipulation of Toxoplasma gondii. In Toxoplasma Gondii; Academic Press: Cambridge, MA, USA, 2007; pp. 391–418.
41. Zhang, C.; Hu, H. High-efficiency nuclear transformation of the diatom Phaeodactylum tricornutum by electroporation. Mar. Genom. 2014, 16, 63–66.
42. McFadden, G.I. Plastids and protein targeting. J. Eukaryot. Microbiol. 1999, 46, 339–346.
43. Roos, D.S.; Crawford, M.J.; Donald, R.G.; Kissinger, J.; Klimczak, L.J.; Striepen, B. Origin, targeting, and function of the apicomplexan plastid. Curr. Opin. Microbiol. 1999, 2, 426–432.
44. DeRocher, A.; Hagen, C.B.; Froehlich, J.E.; Feagin, J.E.; Parsons, M. Analysis of targeting sequences demonstrates that trafficking to the Toxoplasma gondii plastid branches off the secretory system. J. Cell Sci. 2000, 113, 3969–3977.
45. Waller, R.F.; Reed, M.B.; Cowman, A.F.; McFadden, G.I. Protein trafficking to the plastid of Plasmodium falciparum is via the secretory pathway. EMBO J. 2000, 19, 1794–1802.
46. Apt, K.E.; Zaslavkaia, L.; Lippmeier, J.C.; Lang, M.; Kilian, O.; Wetherbee, R.; Grossman, A.R.; Kroth, P.G. In vivo characterization of diatom multipartite plastid targeting signals. J. Cell Sci. 2002, 115, 4061–4069.
47. Sheiner, L.; Demerly, J.L.; Poulsen, N.; Beatty, W.L.; Lucas, O.; Behnke, M.; White, M.W.; Striepen, B. A systematic screen to discover and analyze apicoplast proteins identifies a

conserved and essential protein import factor. PLOS Pathog. 2011, 7, e1002392.

48. Huesgen, P.F.; Alami, M.; Lange, P.F.; Foster, L.J.; Schröder, W.P.; Overall, C.M.; Green, B.R. Proteomic amino-termini profiling reveals targeting information for protein import into complex plastids. PLoS ONE 2013, 8, e74483.
49. Füssy, Z.; Oborník, M. Chromerids and their plastids. In Advances in Botanical Research; Elsevier: Amsterdam, The Netherlands, 2017; Volume 84, pp. 187–218.
50. Oborník, M.; Lukeš, J. Cell biology of chromerids. In International Review of Cell and Molecular Biology; Academic Press: Cambridge, MA, USA, 2013; Volume 306, pp. 333–369.
51. Nielsen, H. Predicting secretory proteins with SignalP. In Protein Function Prediction; Kihara, D., Ed.; Humana Press: New York, NY, USA, 2017; pp. 59–73.
52. Emanuelsson, O.; Brunak, S.; Von Heijne, G.; Nielsen, H.A. Locating proteins in the cell using TargetP, SignalP and related tools. Nat. Protoc. 2007, 2, 953–971.
53. Gruber, A.; Rocap, G.; Kroth, P.G.; Armbrust, E.V.; Mock, T. Plastid proteome prediction for diatoms and other algae with secondary plastids of the red lineage. Plant J. 2015, 81, 519–528.
54. Füssy, Z.; Faitová, T.; Oborník, M. subcellular compartments interplay for carbon and nitrogen allocation in Chromera velia and Vitrella brassicaformis. Genome Biol. Evol. 2019, 11, 1765–1779.
55. Fukasawa, Y.; Tsuji, J.; Fu, S.-C.; Tomii, K.; Horton, P.; Imai, K. MitoFates: Improved prediction of mitochondrial targeting sequences and their cleavage sites. Mol. Cell. Proteom. 2015, 14, 1113–1126.
56. Gruber, A.; McKay, C.; Kroth, P.G.; Armbrust, E.V.; Mock, T. Comparison of different versions of SignalP and TargetP for diatom plastid protein predictions with ASAFind. Matters 2020, 81, 519–528.